V.V. Shchennikov, I.V. Korobeynikov, N.V. Morozova

Institute of Metal Physics of Russian Academy of Sciences, Urals Division,
18, S. Kovalevskaya Str., Yekaterinburg, 620990, Russia

INFLUENCE OF PHYSICAL AND "GEOMETRICAL" FACTORS ON THE PROPERTIES OF THERMOELECTRIC MATERIALS

In the present work, the ways to improvement of thermoelectric parameters are considered based on exploring both physical and "geometrical" factors. The experimental results on the influence of pressure and magnetic field on thermoelectric properties for a wide range of materials are analyzed. Experimental data are obtained in the pressure range of 0 – 30 GPa using an automated setup with the sintered diamond anvils, and the measurements of the thermo-magnetic Nernst-Ettingshausen effect are carried out using an autonomous version of the diamond anvils cell. The approach has been developed for the calculations of the above mentioned effects for inhomogeneous thermoelectric materials. The results of calculations are found to be in good agreement with the experimental data obtained in the vicinity of semiconductor-metal phase transition. It is shown that both physical and "geometrical" factors can improve the power factor of materials.
Key words: Nernst-Ettingshausen effect, Seebeck effect, high-pressure, multi-phase materials.

Introduction

The basic parameters characterizing performance of thermoelectric (TE) converters are the power factor, and the figure of merit:

$$æ = \frac{S^2}{\rho}, \qquad Z = \frac{S^2}{\rho \cdot \lambda}, \tag{1}$$

depending on the thermopower S, the electrical resistivity ρ, and the thermal conductivity $\lambda = \lambda_e + \lambda_{ph}$ consisting of electron (λ_e) and phonon (λ_{ph}) contributions. All the parameters depend on semiconductor gap E_g. The ways to improvement of the above thermoelectric parameters are considered based on exploring both physical factors including high pressure and magnetic fields and "geometrical" factors, like configuration and concentration of discrete elements of multi-phase thermoelectric material.

Experimental details and results

Experimental thermoelectric data were obtained using two automated setups with diamond and hard alloy high pressure anvils [1]. An automated high-pressure setup made it possible to measure simultaneously the force applied, the sample thickness, anvil temperature, thermal gradient ΔT, and electrical signal from the sample [2-3].Temperature distribution in the anvils for various sample sizes and thermal conductivities [2-3] was used for estimation of error in the determination of ΔT along the sample. The measurements of thermomagnetic Nernst-Ettingshausen (N-E) effect were performed using miniature versions of high-pressure chambers with sintered diamond anvils in the stationary magnetic field up to $B \sim 2$ T. New results, as well as those published earlier, were considered in the range of pressures up to ~ 40 GPa.

Influence of physical factors on the thermoelectric parameters of materials: high pressure

A typical variation of the electrical resistivity ρ, the thermal conductivity λ and the thermoelectric power S versus a change in forbidden gap E_g is shown in Fig. 1. The dependences reflect the complex behavior of the above values on E_g which is mainly due to variation of the concentration and mobility of charge carriers. As a result, TE parameters æ and Z have the optimal values in the certain range of E_g values (Fig. 1). The above figure explains high TE properties of narrow-gap semiconductors like Bi_2Te_3, $PbTe$, etc. and also serves as an indicator in searching for novel materials for TE applications. At the same time, Fig. 1 shows that variation of E_g either from large values or from zero ones under some exposure may bring the material into the region of optimal values of E_g for thermoelectricity. High pressure seems to be such an exposure due to strong influence on E_g both in the region of structural stability [4] and in the vicinity of phase transition which leads to opening of E_g or its drastic variation.

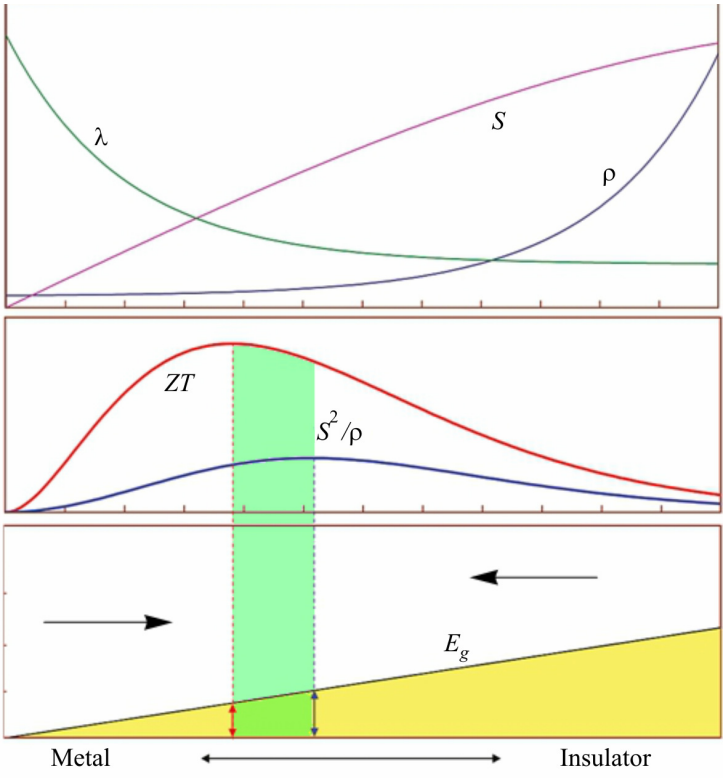

Fig. 1. Dependences of the thermopower (S), the electrical resistivity (ρ), the thermal conductivity (λ), the thermoelectric power factor æ and dimensionless figure of merit (ZT) on the energy gap. The maxima of æ and (ZT) are achieved at some optimal values of a forbidden gap (shown by vertical arrows and by dashed lines). The right and left arrows show that the above optimal values of E_g can be achieved either by decreasing the semiconductor gap (right arrow) or by opening it (left arrow) due to applied pressure.

The pressure dependence of thermoelectric power S can be described by an equation valid for a nearly intrinsic semiconductor [1, 5]:

$$\frac{S}{k/|e|} = \left\{ \sum_i \frac{(\sigma_{pi} - \sigma_{ni})}{\sigma} \times (r+2) + \sum_i \frac{(\sigma_{pi} - \sigma_{ni})}{\sigma} \times \frac{E_g}{2kT} + \frac{3}{4} \times \ln \frac{m_p^*}{m_n^*} + \frac{\Delta E_v}{kT} \times \frac{\sigma_{p2}}{\sigma} \right\}, \qquad (2)$$

where $\sigma = \Sigma(\sigma_{ni} + \sigma_{pi})$ is the total conductivity, $m_p^*(m_n^*)$ is the effective masses of holes (electrons), and r is the scattering parameter of carriers, ΔE_v is the energy difference between the upper and the next bands.

The index "*i*" corresponds to the electron and hole bands, and the index "2" corresponds to the additional hole band, like in Bi_2Te_3 and *PbTe* [5]. The variation of both E_g and ΔE with *P* affects the value of *S*.

The value of *S* corresponds to the average energy transferred by electrons (term ~ E_g) and depends both on the position of the Fermi level (term ~ $\ln(m_p/m_n)$) and on the contribution of second valence band (term ~ ΔE_v).

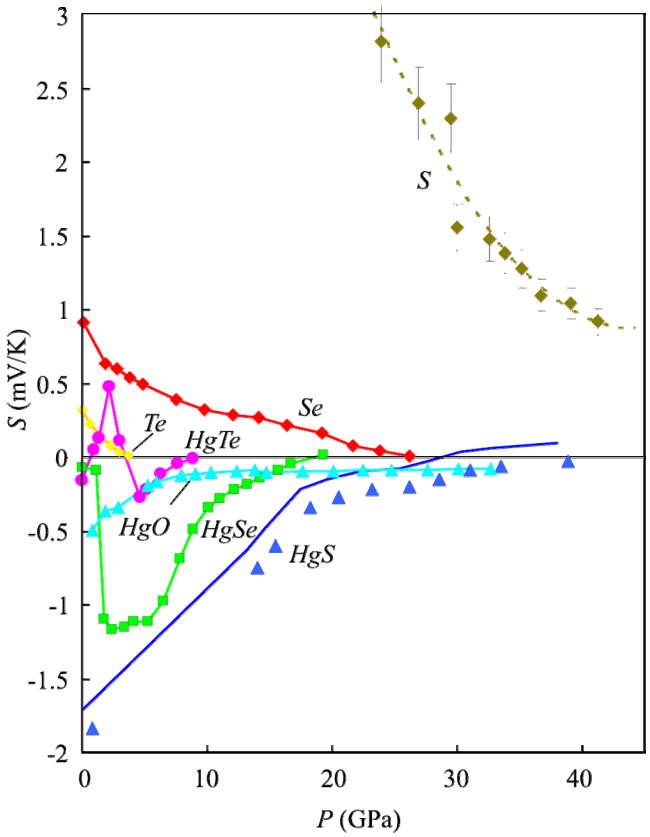

Fig. 2. Thermoelectric power of mercury chalcogenides and chalcogens at very high pressures. The curves virtually demonstrate the variation of energy gaps in a wide range of pressures, since the value of S is proportional to E_g (Eq. 2). The data for HgTe, HgSe, HgS, Te, and Se are taken from [2], the data for HgO are from [6] and for sulphur – from [7].

Fig. 2 shows *S*(*P*) dependence for mercury chalcogenides and chalcogens in a wide pressure range, reflecting the behavior of E_g. For *Te*, *Se*, cinnabar *HgS*, mercury oxide *HgO* and sulphur *S* a strong decrease in *S* was observed under high pressure, testifying to narrowing of E_g (Fig. 2). The first four materials *Te*, *Se*, *HgS* and *HgO* were found to transfer into metal state with closing of E_g [2, 6]. For gap-less semiconductors *HgTe* and *HgSe* the abrupt opening of E_g was established at pressure-induced phase transition from zinc blende to cinnabar structure [2]. With further increase in pressure *P*, the narrowing of E_g and transition to metal state was also found [9]. In Fig. 3, the results of high pressure application are shown for $Sn_2P_2S_{1-x}Se_x$ crystals in the pressure range of 0 – 22 GPa. Under ambient conditions, Sn_2P_2S-based compounds are known to be ferroelectrics with a wide forbidden gap E_g ~ 2.3 eV [8]. The application of pressure strongly decreases the gap E_g and thus causes the drop of electrical resistance by ~ 8 orders of magnitude (Fig. 3). In the pressure range of ~ 15 – 22 GPa the compounds become narrow-gap semiconductors with acceptable thermoelectric properties (Fig. 3). For a basic crystal SnP_2S_6 the closing of E_g and transition to metal state was confirmed by optical measurements [10] near *P* ~ 39.2 GPa. For mixed $Sn_2P_2S_{6-x}S_x$ compounds with small content of *Se* a similar behavior is expected under pressure.

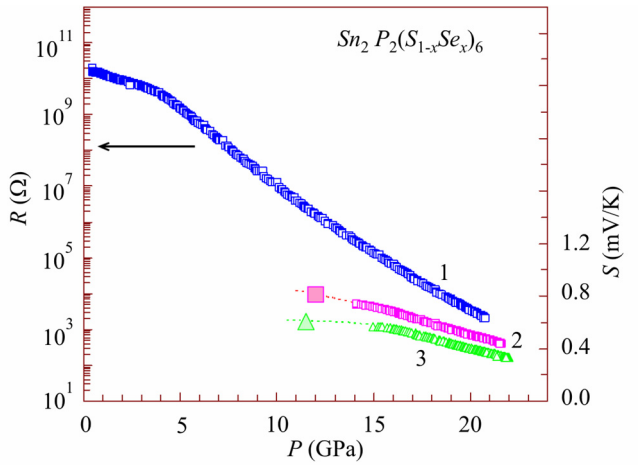

Fig. 3. The pressure dependences of the electrical resistance (1) and the thermoelectric power (2, 3) of $Sn_2P_2(S_{1-x}Se_x)_6$ crystals at room temperature for samples with x = 0.082 (1, 3) and x = 0.092 (2). A series of electronic transitions, starting from a ferroelectric to a paraelectric near ~ 1 GPa, then to a wide-gap semiconductor, and then to narrow-gap semiconductor occurs up at a pressure of 22 GPa. Above ~ 30 GPa the transition to metal state is expected [8].

Thus, it can be noted that the external pressure is really able to bring wide-gap materials into optimal range of E_g for thermoelectricity. The opposite case of opening E_g due to pressure-induced phase transitions for *HgTe* (Fig. 2), *PbTe* and *PbSe* [11] crystals also shows the improvement of thermoelectric properties. The theoretical calculations confirm that high pressure phases of *HgTe* (above ~ 2 GPa), *PbTe* and *PbSe* (above 5 – 6 GPa) are indeed potentially promising thermoelectrics [12-14].

Influence of physical factors on the thermoelectric parameters of materials: magnetic field

The influence of magnetic field on TE parameters is mainly realized due to longitudinal $\Delta S_{\parallel}$ and transverse Q thermomagnetic N-E effects – thermal analogs of magnetoresistance and the Hall effect, respectively [5]

$$\Delta S_{\parallel}(B) = A_2 \times \left(\frac{k}{e}\right) \times (\mu \times B)^2, \tag{3}$$

$$Q = A_3 \times r \times \left(\frac{k}{e}\right) \times \mu, \tag{4}$$

$$Q = \left(\frac{k}{e}\right) a_r \times \left[r\left(\frac{\sigma_n}{\sigma}\mu_n + \frac{\sigma_p}{\sigma}\mu_p\right) + \frac{\sigma_n \sigma_p}{\sigma^2}(\mu_n + \mu_p)\left(2r + 5 + \frac{E_g}{kT}\right) \right], \tag{4a}$$

where e is the electron charge, k is the Boltzmann constant, $\mu = e \times \tau/m$ is the mobility of charge carriers, m is the effective mass, τ is the relaxation time of charge carriers, and r is the scattering parameter describing a dependence of τ on the electron energy ε, $\tau(\varepsilon) \approx \varepsilon^r$. Eq. 4 corresponds to one type of charge carriers, while Eq. 4a – to two types.

Transverse N-E effect Q is proportional to mobility. According to Eqs (3-4), the highest N-E effect ought to arise in materials with the largest mobilities of charge carriers. Combined effect of pressure and magnetic field leads to increasing TE parameters for the pressure-induced states with a negligible direct semiconductor gap. Such states were proved to exist for *Te* and *Se* in the vicinity of

the semiconductor gap closing (Fig. 2) and for *PbTe* and *PbSe* at high pressures near $P \sim 3$ GPa due to decreasing E_g with pressure [15]. Experimental investigations indeed showed a large transverse N-E effect in *Te*, *Se* (Fig. 4) and *PbTe* (Fig. 5) near pressure-induced gap-less states which led to additional increase in power factor (for *PbTe* by ~ 30 % in a magnetic field up to ~ 2 T (Fig. 5)). It would be interesting to test direct-gap $Sn_2P_2S_6$ crystals and compounds on their basis in the vicinity of pressure-induced closing of E_g in the search for strong N-E effects (Fig. 3 and [10]).

Thus, combined application of pressure and magnetic field converts the non-thermoelectric materials like *Te* and *Se* into potential thermoelectric (thermomagnetic) ones. For the known narrow-gap thermoelectric like *PbTe* magnetic field with the simultaneous assistance of high pressure leads to additional increase of TE parameters (power factor, Fig. 5).

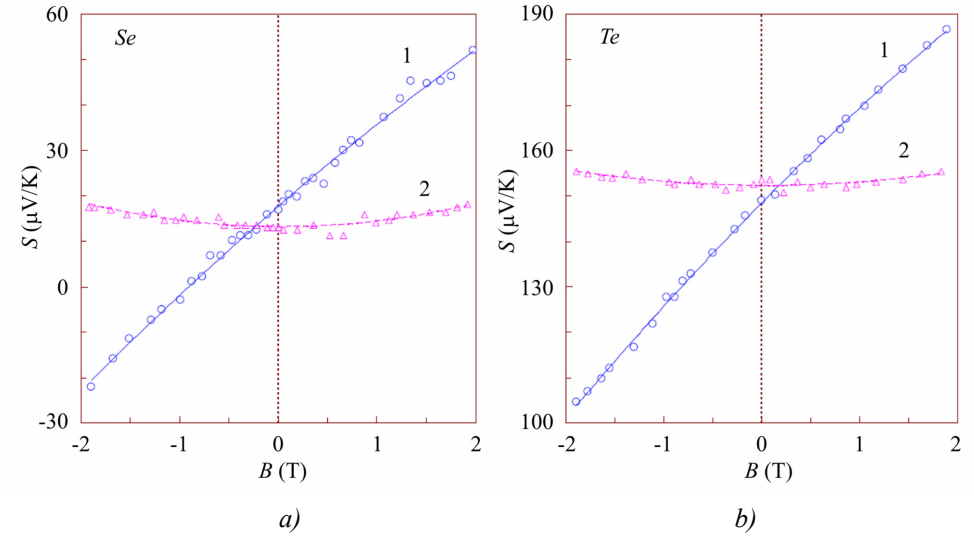

Fig. 4. The magnetic field dependences of thermoelectric power for Se(a), and Te(b) samples in two positions 1 and 2 of high pressure chamber in a magnetic field at fixed pressure, GPa: (a) P = 13.6 GPa; (b) P = 1 GPa.[16]. Position 1 corresponds to transverse N-E effect (Eq. 4), while position 2 – to longitudinal one (Eq. 3). For PbTe samples the similar dependences were obtained and used in the calculation of power factor (see Fig. 5 below).

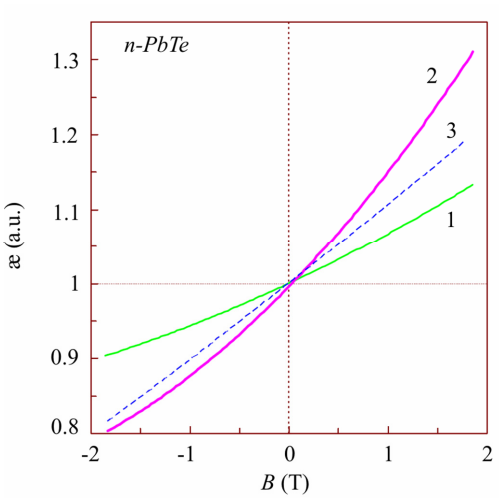

Fig. 5. The dependences of a relative change in the thermoelectric power factor æ on magnetic field B, æ(P;B)/æ(P;B = 0) for a single crystal of n-PbTe at fixed pressures P: 1 – P = 2.0 GPa, $S_0 = S(B = 0) = -190$ μV/K; 2 – P = 3.2 GPa, $S_0 = -127$ μV/K; 3 – P = 4.5 GPa, $S_0 = -79$ ΔV/K[17].

Influence of "geometrical factors" on the thermoelectric parameters of materials

Usually, one can determine experimentally only the generalized characteristics of material (averaged over the total volume of substance measured). These effective properties comprise "geometrical" parameters of every phase: concentration, shape, and position of inclusions [18]. Effective properties of materials (thermal, magnetic, mechanical, etc.) are calculated mostly by two main approaches: in the first one local properties of system are supposed to be known functions of coordinates, and in the second one they are considered statistically as random fields [19].

In the authors' model, the effective electrical resistivity ρ or the electrical conductivity σ (and the thermal conductivity) are considered as normalized sums of phase contributions in two equivalent considerations of "series" and "parallel" electrical (thermal) connection of phases [20, 21]

$$\rho = \sum c_i \rho_i g_i(\rho) \left(\sum c_i g_i(\rho)\right)^{-1}, \tag{5}$$

$$\sigma = \sum c_i \sigma_i g_i(\sigma) \left(\sum c_i g_i(\sigma)\right)^{-1}, \tag{6}$$

where a sum of phase concentrations c_i is equal to 1 and configuration parameters g_i along electrical (thermal) current are of the form:

$$g_i(\rho) = 3/\left[A\rho + (3-A)\rho_i\right] \quad g_i(\sigma) = 3/\left[A\sigma_i + (3-A\sigma)\right] \tag{7}$$

When parameter A equals 0, 3 or 1, the Eq. 5 – 6 agree with the cases of parallel and series electrical connections, or with the case of spherical inclusions, respectively [20-23]. Intermediate values of A ($0 < A < 3$) correspond to interpolated configuration of inclusions in a certain direction (like elongated or contracted ellipsoids).

Unlike the majority of previous models [18, 22, 23] where a shape of inclusions was fixed, in the present model [20] a configuration parameter of phase inclusions is variable between the limiting cases of parallel and series (electrical, thermal) connections. The second distinct advantage of the model is a simultaneous consideration of more than one property of inhomogeneous material.

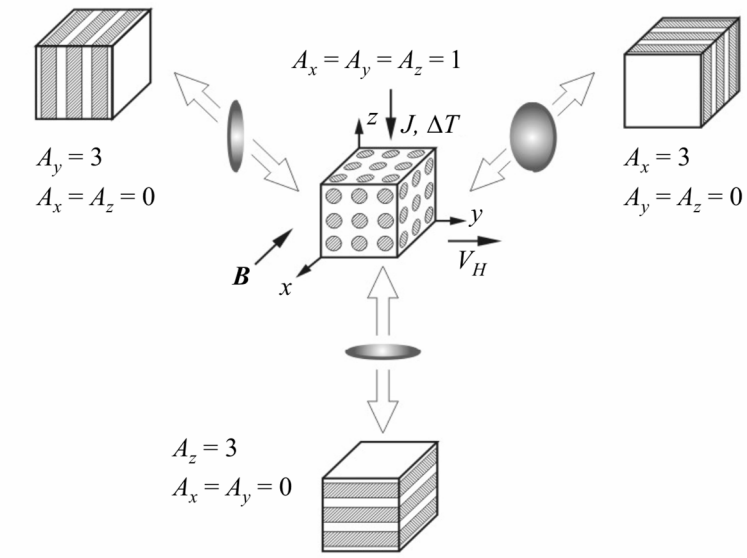

Fig. 6. Examples of materials with the boundary configurations of phase inclusions (planes and spheres). The black arrows show directions of electrical current J (thermal gradient ΔT), magnetic field B and the resulting voltage V_H of the transverse N-E and Hall effects. Parameter A_i along different axes is given for the fixed limiting cases. The intermediate values of A < 1 correspond to elongated ellipsoids, while the values of A > 1 correspond to oblate ones.

As is evident (5) – (7), for the description of effective properties of phase mixture with an arbitrary configuration of inclusions the well-known formulas for parallel and series connection of elements can be used:

$$\sigma^{\parallel} = \sum_{i=1}^{n} \sigma_i c_i \ , \ \sigma^{\perp} = \left(\sum_{i=1}^{n} \frac{\sigma_i}{c_i} \right)^{-1} , \tag{8}$$

on the assumption that voltages (in the first case) and currents (in the second case) for each phase comprise additional multipliers G_i being a function of concentration and configuration of inclusions: $G_i(\rho) \equiv G_i$ and $G_i(\sigma)$

$$G_i = g_i (\sum c_i g_i)^{-1} , \tag{9}$$

$$G_i(\sigma) = g_i(\sigma) \cdot (\sum c_i g_i(\sigma))^{-1} . \tag{10}$$

This approach allows obtaining algebraic formulas for complex properties depending on the vectors of electrical, thermal and magnetic fields directed along the different axes [21]. The application of the approach for the calculation of the electric, thermal, mechanical and magnetic effects is shown below. Interpolation of formula for S obtained in [24, 25] for spherical inclusions to the above simplest limiting cases yields the following equation [20] for a varied configuration of inclusions:

$$S = (\sum S_i c_i g_i(\rho) g_i(\lambda)) / (\sum c_i g_i(\rho) g_i(\lambda)). \tag{11}$$

Eq. (5), (6) and (11) imply a simple relation for the electrical and thermal values of a two-phase system derived for the first time in [20]:

$$\frac{S - S_2}{S_1 - S_2} = \frac{(\rho\lambda - \rho_2\lambda_2)}{(\rho_1\lambda_1 - \rho_2\lambda_2)}. \tag{12}$$

It is interesting that Eq. 12 allows estimating thermoEMF for any system (including modern nano-structures) without cumbersome numerical calculations taking into account certain configuration and concentration of inclusions. The only values required are the effective resistivity and the effective thermal conductivity of the system determined by Eq. 5 and Eq. 6 and the corresponding values of ρ, S and λ for the initial phases. In Fig. 7, the calculated dependences of electrical resistivity and thermoEMF on the concentration of one phase (Eqs. 5, 6), as well as the dependence between them (Eq. 12) are shown for a two-phase system with a variable configuration parameter. The Eq. 12 fits well the experimental data for the materials undergoing semiconductor-metal transitions under pressure or temperature variation [20].

Later in the framework of the model (Fig. 6) a more regular equation for S was obtained [20], to correct the case of spherical inclusions [24, 25]

$$S = (\sum_i S_i \cdot c_i \cdot f_i \cdot (\rho) \cdot \lambda_i^{-1} \cdot f_i(\lambda)) / (\sum_i c_i \cdot f_i \cdot (\rho) \cdot \sum_i c_i \cdot \lambda_i^{-1} \cdot f_i(\lambda)) . \tag{13}$$

For two-phase statistically inhomogeneous materials the equation for S was also obtained in [26], and compared to the equations obtained in [24, 25] for the case of spherical inclusions. For certain binary mixtures the difference between the calculated values of S obtained by these equations (Eq. 11 at $A = 1$) and the equation derived in [26] was estimated to be rather appreciable [26], so correction of Eq. 11 seems to be quite appropriate.

Using Eq. 13 leads to some deviation from the relation (12), especially in the vicinity of the

abrupt change in the properties (near phase transition point), in the case when the thermal conductivities λ_i of phases sufficiently differ. However, for nearly similar thermal conductivities of different phases (components of multi-phase system) Eq. 12 remains sufficiently valid. Due to a wide use of inhomogeneous materials (grain-oriented, textured alloys, etc) in thermoelectricity [27] the relation (12) seems to be useful for the prediction of their properties and, thus, for the development of complex thermoelectric materials.

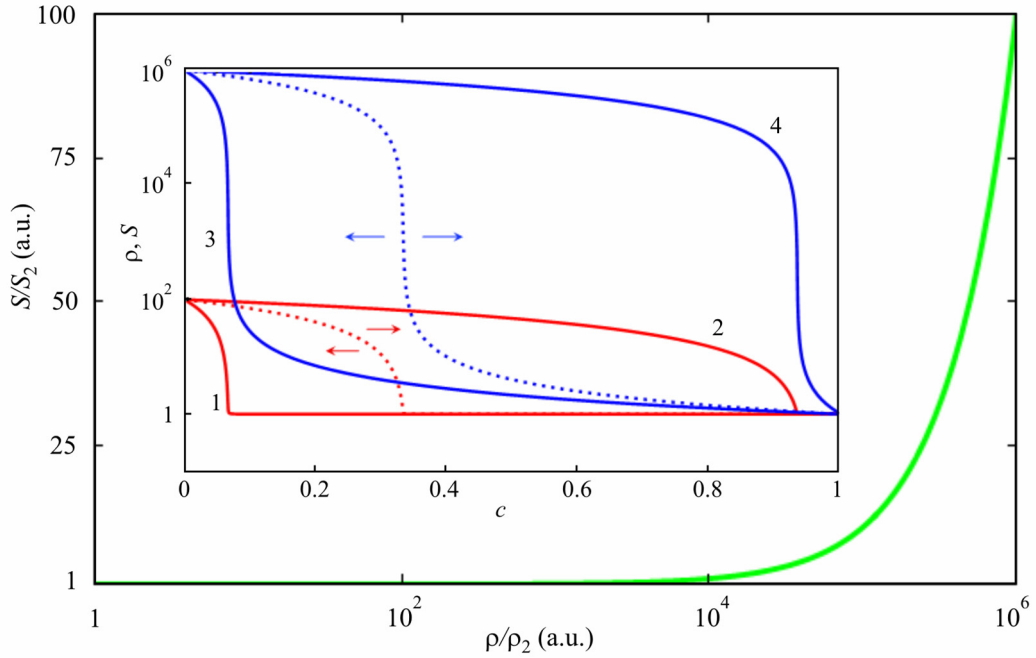

Fig. 7. The relation between the thermopower (S) and the electrical resistivity (ρ) of a two-component system corresponding to Eq. 12 (The parameters of phases taken are as follows $S_1 = 10^2$, $S_2 = 1$, $\rho_1 = 10^6$, $\rho_2 = 1$ a.u.). On the insert, the calculated dependences $S = S(c_1)$ (curves 1 – 2) and $\rho = \rho(c_1)$ (curves 3-4) of a two-component heterophase system on concentration c_1 of component I are shown. Curves 1 and 3 represent the case of A = 0.2 ("nearly parallel" connection) and curves 2 and 4 – A = 2.8 ("nearly series" connection). Dashed curves represent the dependences for parameter A = 1. Arrows show a displacement of the above dependences with increase or decrease in constant A. The drastic drop of thermopower and resistivity values occurs near the concentration c = A/3 of the "metallic" component according to Eqs. 5 and 11.

Developing this model for the transverse N-E effect Q and the Hall effect R for a hetero-phase system, one can obtain [21]:

$$R = \frac{\sum_i c_i \cdot R_i \cdot g_i^J(\sigma) \cdot g_i^H(\rho)}{\left(\sum_i c_i \cdot g_i^J(\sigma)\right) \cdot \left(\sum_i c_i \cdot g_i^H(\rho)\right)}, \quad Q = \frac{\sum_i c_i \cdot Q_i \cdot g_i^T(\lambda) \cdot g_i^H(\rho)}{\left(\sum_i c_i \cdot g_i^T(\lambda)\right) \cdot \left(\sum_i c_i \cdot g_i^H(\rho)\right)}, \tag{14}$$

where g_i^T (g_i^J) and g_i^H are configuration parameters of inclusions along thermal gradient ΔT (current J) and along the Hall direction V_H (perpendicular to magnetic field B), respectively. The parameters A_i are can be varied between the limiting cases of inclusions. Equations (14) coincide with the known formulas for the limiting cases of layered structures [28]. By the way, the equation for Young's modulus was also derived with the use of this model [21], which demonstrated good agreement with the experimental data, including the case of hard alloys in a wide range of component concentrations [29].

Thermoelectric power factor (æ) and thermoelectric figure of merit (Z) of a hetero-phase system

are also functions of concentration and geometrical configuration of inclusions (Fig. 8). Calculations performed using Eqs. 5, 6 and Eq. 13 for some two-phase systems (Fig. 8) show that thermoelectric power factor æ exceeds significantly the values of æ of each component. Losing a little in the thermoelectric figure of merit, one can increase considerably the thermoelectric power factor for "nearly layered" configuration of components (curve 1 in Fig. 8). Note, that at HP-HT synthesis or treatment resulting in production of inhomogeneous materials (grain-oriented, textured alloys, etc), the increase in power factor is really achieved in some cases [27].

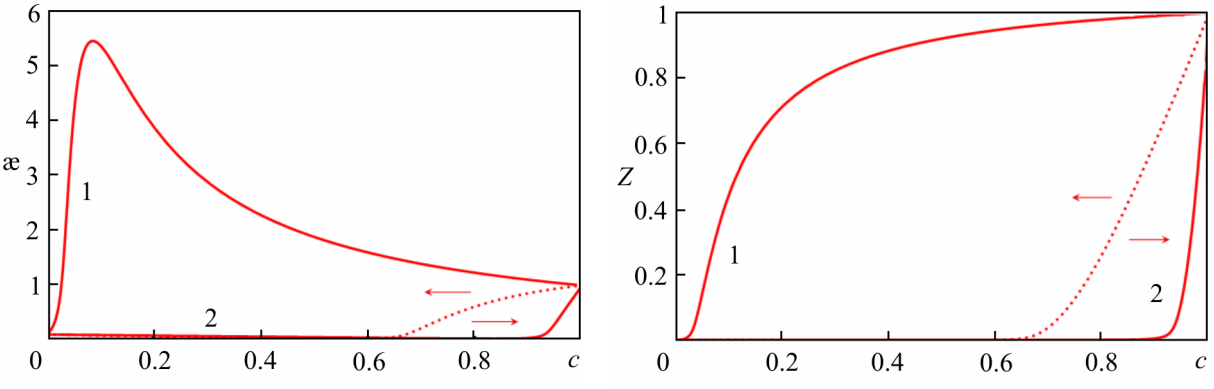

a) *b)*

Fig. 8. Dependence of normalized thermoelectric figure of merit Z (right) and thermoelectric power factor æ *(left) of a two-phase system on concentration c_1 of phase I calculated by Eq. 5, 6 and Eq. 13 ($\lambda_1 = 1$, $\lambda_2 = 100$, $\rho_1 = 10^4$, $\rho_2 = 1$, $S_1 = 100$, $S_2 = 1$ a. u.). The parameter A is taken to be A = 2.9 (curves) 1) and A = 0.2 (curves 2). For dashed curves A = 1. The arrows show a displacement in the dependences with decrease or increase of A.*

Magnetic field can further improve the thermoelectric parameters æ, *Z* characterizing the work of thermoelectric cooling devices, as thermo-magnetic cooling by N-E effect is known to be preferable in comparison with the pure Peltier one [27]. Thus, the approach developed allows to improve working parameters of thermoelectric generators, as well as to take into account the parasitic signals caused by the N-E and Hall effects in operation of electronic devices.

Conclusion

The ways to improvement of thermoelectric parameters through use of physical factors including high pressure and magnetic field, as well as "geometrical" ones including configuration and concentration of discrete elements of a multi-phase thermoelectric material are considered.

High pressure was shown to improve TE parameters of some substances due to variation of semiconductor gap E_g in a wide range, and the narrowing or opening of E_g. Certain non-TE materials, as well as high-pressure phases were found to be promising thermoelectrics.

A combined effect of high pressure and magnetic field is capable of improving TE parameters of substances in pressure-induced narrow-gap and gap-less states with very high mobilities of charge carriers and strong N-E effects.

Variation of the concentration and configuration of discrete elements of a multi-phase system seems incapable of improving the figure of merit by simple "mixing" of phases, but the power factor can strongly increase due to optimal choice of "geometrical" factors.

Acknowledgments. The work was done within RAS Program (Project no. 01.2.006 13394), by UD RAS as part of Program ''Matter at high energy densities'' of the Presidium of RAS (project 12-P-2-1004), by the Ministry of Education and Science of the Russian Federation (Contract 14.518.11.7020), and by the Oriented Basic Research Project of the Ural Branch of the Russian Academy of Sciences.

References

1. V.V. Shchennikov, S.V. Ovsyannikov, and A.Y. Manakov, Measurement of the Seebeck Effect (Thermoelectric Power) at High Pressure up to 40 GPa, *J. Phys. Chem. Solids* **71**, 1168 – 1174 (2010).
2. I.M. Tsidil'kovskii, V.V. Shchennikov, and N.G. Gluzman, Thermoelectric Power of Mercury Chalcogenides at Very High Pressures, *Semiconductors* **17**, 604 – 606 (1983).
3. V.V. Shchennikov, S.V. Ovsyannikov, Phase Transitions from Mechanical Contraction: Direct Observation of Phase-Transition-Related Volumetric Effects in Crystals of *ZnO*, *GaAs*, $CaCO_3$, and *CeNi* under Compression up to 25 GPa, *High Pressure Res*. **29**, 514 – 519 (2009).
4. W. Paul, D.M. Warshawer, *Solids under Pressure* (New York, McGraw-Hill, 1963), 524.
5. B.M. Askerov, *Electron Transport Phenomena in Semiconductors* (Singapore, World Scientific, 1994), 416.
6. I.M. Tsidil'kovskii, V.V. Shchennikov, and N.G. Gluzman, Influence of Ultrahigh Pressures on the Electrical Properties of Mercury Oxide, *Semiconductors* **19**, 901 – 902 (1985).
7. V.V. Shchennikov, S.V. Ovsyannikov, Thermoelectric Power of Sulphur at High Pressure up to 40 GPa, *Phys. Status Solidi (b)* **239**, 399 – 404 (2003).
8. V.V. Shchennikov, N.V. Morozova, I. Tyagur, Y. Tyagur, and S.V. Ovsyannikov, Colossal Tuning of an Energy Gap in $Sn_2P_2S_6$ under Pressure, *Appl. Phys. Lett*. **99**, 212104 (2011).
9. I.M. Tsidil'kovskii, V.V. Shchennikov, and N.G. Gluzman, Metallization of Mercury Chalcogenides under Ultrahigh Pressures, *Physics of the Solid State* **24**, 1507 – 1511 (1982).
10. S.V. Ovsyannikov, H. Gou, N.V. Morozova, I. Tyagur, Y. Tyagur, and V.V. Shchennikov, Raman Spectroscopy of Ferroelectric $Sn_2P_2S_6$ under High Pressure up to 40 GPa: Phase Transitions and Metallization, *J. Appl. Phys*. **113**, 013511 (2013).
11. S.V. Ovsyannikov, V.V. Shchennikov, Y.S. Ponosov, S.V. Gudina, V.G. Guk, E.P. Skipetrov, and V.E. Mogilenskikh, Application of the High-Pressure Thermoelectric Technique for Characterization of Semiconductor Micro-Samples: *PbX*-Based Compounds, *J. Phys. D: Appl. Phys.* **37**, 1151 – 1157 (2004).
12. S.V. Streltsov, A.Yu. Manakov, A.P. Vokhmyanin, S.V. Ovsyannikov, and V.V. Shchennikov, Crystal Lattice and Band Structure of Intermediate High-Pressure Phase of *PbSe*, *J. Phys.: Condens. Matter* **21**, 385501 (2009).
13. Y. Wang, X. Chen, T. Cui, Y. Niu, Y. Wang, M. Wang, Y. Ma, and G. Zou, Enhanced Thermoelectric Performance of *PbTe* within the Orthorhombic Pnma Phase, *Phys. Rev. B* **76**, 155127 (2007).
14. X. Chen, Y. Wang, T. Cui, Y. Ma, G. Zou, and T. Iitaka, *HgTe*: A Potential Thermoelectric Material in the Cinnabar Phase, *J. Chem. Phys*. **128**, 194713 (2008).
15. V.V. Shchennikov, S.V. Ovsyannikov, A.Yu. Derevskov, Thermopower of Lead Chalcogenides at High Pressures, *Phys. Solid State* **44**, 1845 – 1849 (2002).
16. V.V. Shchennikov, S.V. Ovsyannikov, Thermoelectric and Galvanomagnetic Investigations of VI Group Semiconductors *Se* and *Te* at High Pressure up to 30 GPa, *Solid State Commun*. **121**,

323 – 327 (2002).
17. V.V. Shchennikov, S.V. Ovsyannikov, and A.V. Bazhenov, A Composite High-Pressure Cell with Sintered Diamond Insets for Study of Thermoelectric and Thermomagnetic Properties in a Range up to 30 GPa: Application to *Pr* and *PbTe*, *J. Phys. Chem. Solids* **69**, 2315 – 2324 (2008).
18. B. Makhov, B.Z. Pevzner, Influence of the Type of Structure on the Properties of the Heterophase Materials, *Izv. AN USSR: Inorg. Mater*. **21**, 1599 – 1607 (1985).
19. J. Sandetski, *Mechanics of Composite Materials* (New York and London, Academic Press, 1974).
20. V.V. Shchennikov, ThermalEMF and Electrical Conductivity of Materials in the Region of the Semiconductor – Metal Phase Transition Point, *Phys. Met. Metall*. **67**, 92 – 96 (1989).
21. V.V. Shchennikov, S.V. Ovsyannikov, G.V. Vorontsov, and V.V. Shchennikov Jr., Investigations of Multiphase States in Vicinity of Pressure-Induced Phase Transitions, *Phys. Status Solidi (b)* **241**, 3203 – 3209 (2004).
22. V.I. Odelevskii, Calculation of Overall Conductivity of Heterogeneous Systems, *J. Tech. Phys*. **21**, 667 – 685 (1951).
23. R. Landauer, The Electrical Resistance of Binary Metallic Mixtures, *J. Appl. Phys*. **23**, 779 – 784 (1952).
24. S.V. Airapetyants, Thermoelectric Force and the Additional Thermoconductivity of Statistical Mixture, *J. Tech. Phys*. **27**, 478 – 483 (1957).
25. V. Halpern, The Thermopower of Binary Mixtures, *J. Phys. C: Solid State Phys*. **16**, L217 – L220 (1983).
26. C. Herring, Effect of Random Inhomogeneties on Electrical and Galvanomagnetic Measurements, *J. Appl. Phys*. **31**, 1939 – 1953 (1960).
27. S.V. Ovsyannikov, V.V. Shchennikov, High-Pressure Routes in the Thermoelectricity or How one Can Improve a Performance of Thermoelectrics, *Chem. Mater*. **22**, 635 – 647 (2010).
28. G.N. Dul'nev, V.V. Novikov, *Transfer Processes in Inhomogeneous Media* (Leningrad, Energoatomizdat, 1991), 248.
29. S.V. Ovsyannikov, V.V. Shchennikov, I.A. Komarovskii, G.V. Vorontsov, I.V. Korobeynikov, and V.V. Shchennikov Jr., Electrical and Mechanical Properties of Multi-Phase Systems under External Impacts, *Proc. SPIE 7978*, 79781W (2011).

Submitted 04.06.2013.